OBJECTIVES

The objectives of the SASI Spatial Analysis were to (1) explore the spatial structure of the asymptotic area swept (z_∞), (2) define clusters of high and low z_∞ for each gear type, (3) determine the levels of z_∞ in present and candidate management areas relative to the model domain, and (4) identify the areas of equal size with z_∞ values similar to or higher than the tested areas. Objectives 1 and 2 were addressed using Local Indicators of Spatial Association (LISA) statistics, while objectives 3 and 4 were addressed using an Equal Area Permutation (EAP) approach.

z_∞ Spatial Structure and Clusters

Methods

The Local Indicators of Spatial Association (LISA) statistics developed by Anselin (1995) are designed to test individual sites for membership in clusters. These tools differ from commonly used global statistics such as Moran's I, Geary's c, and Matheron's variogram which are designed to describe the general autocorrelation characteristics of a pattern. Cressie's (1993) "pocket plot" can identify outliers, but does not provide a formal test of significance. Variograms can dissect patterns into their directional components, but are not designed for single spatial foci as are local statistics.

LISA statistics including Moran Scatterplots and Local Moran's *I* were used to explore the spatial structure of z_∞ and to determine if each SASI grid cell is a member of a high or low z_∞ accumulation cluster. The LISA analysis for each SASI grid cell (1) indicates the extent of significant spatial clustering of similar values around that cell, and (2) the sum of LISAs for all cells is proportional to a global indictor of spatial association (Anselin 1995).

For exploratory spatial data analysis Global Moran's *I* was used to determine the general level of spatial autocorrelation in the data. *I* is an index of linear association between a set of spatial observations x_i x_j, and a weighted average w_{ij} of their neighbors (Moran 1950):

$$I = \frac{n}{\displaystyle\sum_{i=1}^{n}\sum_{j=1}^{n} w_{i,j}} \cdot \frac{\displaystyle\sum_{i=1}^{n}\sum_{j=1}^{n} w_{i,j} x_i x_j}{\displaystyle\sum_{i=1}^{n} x_i^2},$$

where $x_i = z_{\infty i} - \overline{Z_\infty}$, $z_{\infty i}$ is the asymptotic area swept accumulated in cell i, and $\overline{Z_\infty}$ is the overall mean asymptotic area swept accumulated in the entire model domain. The neighborhood weights, $w_{i,j}$, were determined using Queen Contiguity, also known as

the 8-neighbor rule (Fortin and Dale 2005). Moran's $I > 0$ indicates that the z_∞ values in the model domain are positively autocorrelated, while $I < 0$ indicates negative autocorrelation. When $I = 0$ the values are spatially random.

The spatial association of each cell with its neighbors was estimated with the Local Moran's I_i (Anselin 1995):

$$I_i = \frac{x_i}{Q_i^2} \sum_{j=1, j \neq i}^{n} w_{i,j} x_i,$$

where

$$Q_i^2 = \frac{\sum_{j=1, j \neq i}^{n} w_{i,j}}{n-1} - \overline{X}^2.$$

When $I_i > 0$ there is positive local autocorrelation, i.e., the cell is in a neighborhood of cells with similar characteristics, but which deviate (positively or negatively) from the overall mean cell characteristics $\overline{X}^2 (= \overline{Z_\infty})$. Negative autocorrelation ($I_i < 0$) occurs when the cell is in a neighborhood with dissimilar z_∞ characteristics. When $I_i = 0$ the cell is in a neighborhood with random characteristics, or when the cell and its neighbors have characteristics equal to the overall mean (Boots 2002).

A Moran scatterplot is a bivariate plot of w_i as a function of x_i, and the slope of a line fit to the scatterplot gives global Moran's I (Anselin 1996). The four quadrants of the scatterplot indicate an observation's value relative to its neighbors with cluster significance defined by the p-values associated with each cell's I_i. Cells with higher than average values ($x_i > 0$) with neighboring high values ($w_i > 0$) are in the High-High quadrant, and together with those in the Low-Low ($x_i < 0$, $w_i < 0$) quadrant indicate positive local spatial autocorrelation. The High-Low and Low-High quadrants indicate negative local spatial autocorrelation. Because the objective of this spatial analysis is to identify clusters of high z_∞, the High-High (H-H) and High-Low (H-L) clusters were mapped.

Local spatial statistics are particularly susceptible to Type I errors when the data are globally autocorrelated because multiple comparisons are being made among many values, some of which are clearly not independent (Ord and Getis 2001, Boots 2002). Ord and Getis (2001) state "*if tests are applied without regard to global autocorrelation structure, Type I errors may abound. That is, locations are identified as hot spots simply because they lie in areas of generally high (or low) values.*" Applying typical multiple comparison corrections (e.g. Sidak or Bonferonni) to the 2,600 cells compared in the SASI model

domain results in extreme criteria for significance (i.e., $p < 1 \times 10^{-6}$). However, not all samples in the data set are correlated to all others so these corrections are far too conservative (Boots 2002). When global autocorrelation was evident ($I \neq 0$) Ord and Getis (2001) suggest using the significance tests in "*informal search procedures rather than formal bases for inference*". Therefore, a range of p-values ($p \leq 0.1$, 0.05, and 0.01) were examined as the criteria for systematically defining clusters of z_∞. Global autocorrelation in z_∞ values influences these tests.

Results

z_∞ Spatial Structure and Clusters

Asymptotic area swept (z_∞) for all gear types demonstrated strong global spatial autocorrelation ($I > 0$, $p \leq 0.0001$, Table 1).

Table 1 - Global Morans *I* statistic and p-value for each gear type.

| Gear	Global Morans *I*	*p*
Trawl	0.4748	≤0.0001
Dredge	0.4650	≤0.0001
H. Dredge	0.8281	≤0.0001
Gillnet	0.4029	≤0.0001
Longline	0.4052	≤0.0001
Trap	0.6868	≤0.0001

The Moran scatterplots show the degree of global spatial autocorrelation for each gear type and identify the quadrant location of every cell and neighborhood in the domain (Figure 1).

Figure 1 – Moran scatterplots for each gear type.
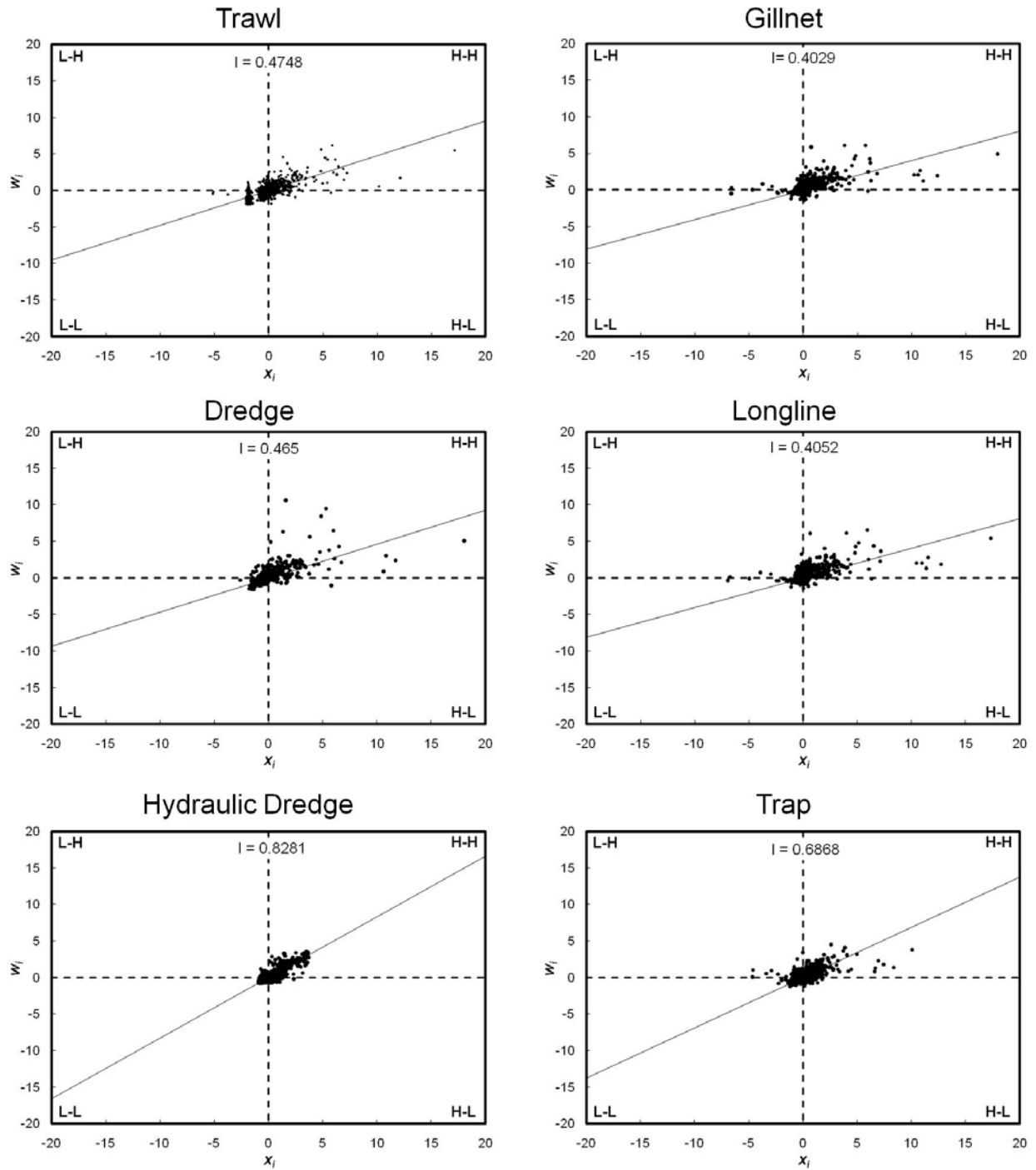
The different gear-specific depth limits used in SASI result in different connectivity between cells in the model (i.e. more or less edge). Reduced connectively (fewer neighbors) impacts cluster identification. The distribution of connections was similar between gear types and in all cases more than 60% of cells had 8 neighbors and 90% had at least 4 neighbors indicating that cluster identification was consistent between gear types (Figure 2).

Figure 2 – Connectivity histograms show the number of cells by number of neighbors for each gear type
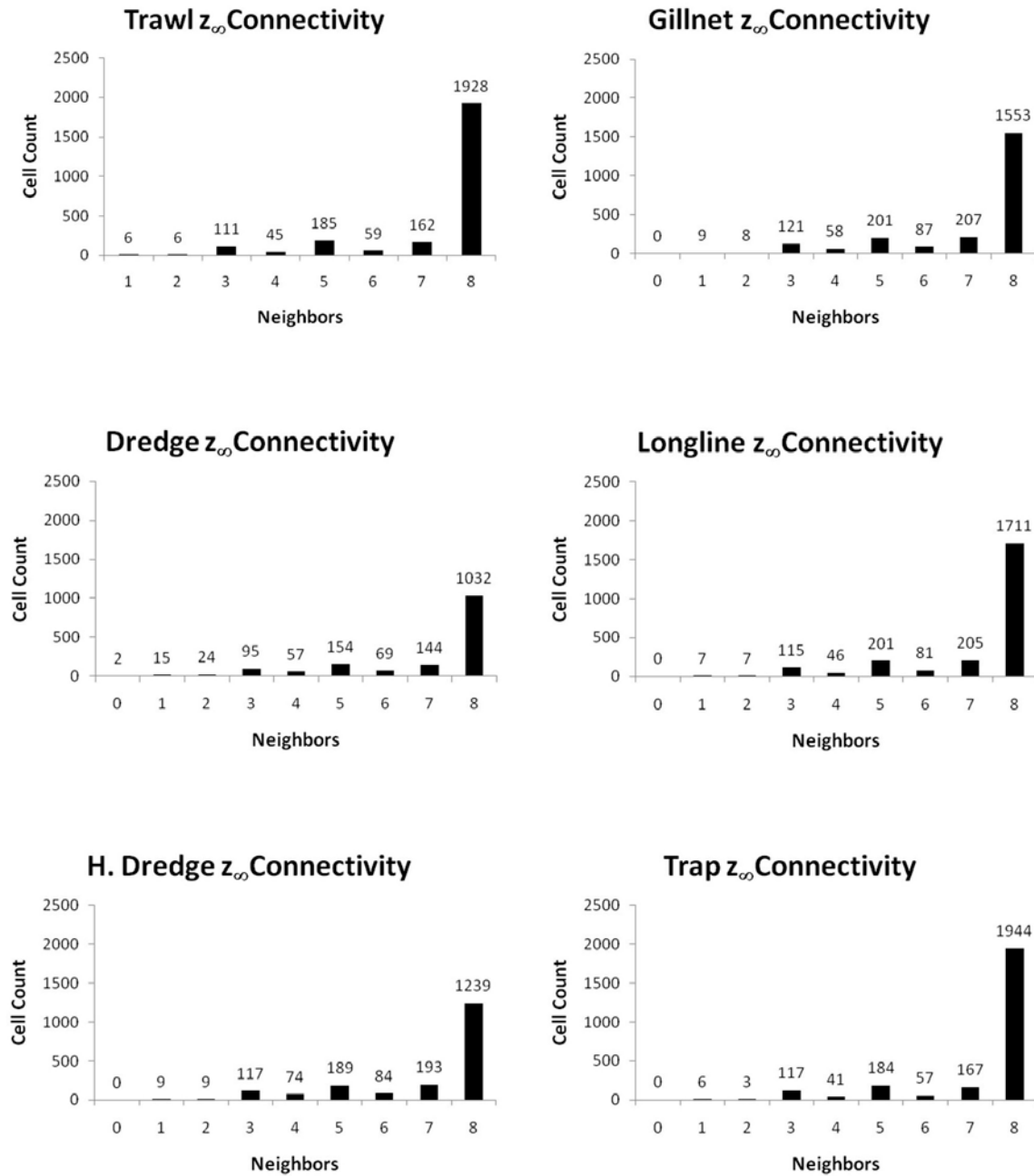
The LISA analysis delimited clusters of high and low z_∞ for all gear types at the $p \le 0.1$, 0.05 and 0.01 levels. Using $p \le 0.1$ criteria resulted in clusters which were nearly identical to $p \le 0.05$ (11 additional cells, see Figure 3) so only $p \le 0.05$ and 0.01 results are presented in Figure 4 and Figure 5. Regardless of gear type, most of the cells in the model did not form significant clusters (Figure 4). Where clustering occurred, between 85 and

99% of cells were in Low-Low or High-High clusters consistent with strong spatial autocorrelation. Outliers (High-Low and Low-High) were rare.

There were seven clusters identified for both trawls and scallop dredges which were larger than 300 km². These clusters correspond to named features (Table 2 and Table 3).

**Table 2 – The name, mean z∞, sum z∞, and the area of each p ≤ 0.01 cluster greater than 300 km²
identified for Trawl gear.**

	Trawl *p* ≤ 0.01			
Number	**Name**	**Mean z∞**	**Sum z∞**	**km²**
1	South of Mt Desert Island Cluster	67.828	474.797	470
2	Jeffrey's Bank Cluster	60.898	487.185	800
3	Platts Bank Cluster	57.369	917.911	1600
4	Cape Neddick Cluster	51.416	154.247	283
5	Georges Shoal Cluster	57.404	746.251	1300
6	Great South Channel Cluster	55.580	833.696	1500
7	Brown's Ledge Cluster	55.785	223.138	273

**Table 3 – The name, mean z∞, sum z∞, and the area of each p ≤ 0.01 cluster greater than 300 km²
identified for Dredge gear.**

	Dredge *p* ≤ 0.01			
Cluster	**Name**	**Mean z∞**	**Sum z∞**	**km²**
1	South of Mt Desert Island Cluster	77.805	311.222	182
2	Jeffrey's Bank Cluster	-	-	-
3	Platts Bank Cluster	68.593	137.186	200
4	Cape Neddick Cluster	58.058	58.058	87
5	Georges Shoal Cluster	59.805	717.656	1200
6	Great South Channel Cluster	58.432	934.908	1600
7	Brown's Ledge Cluster	58.155	232.621	273

Figure 3 – Maps of z_∞ H-H and H-L clusters defined by $p \leq 0.1$, 0.05 and 0.01 levels for otter trawl gear.
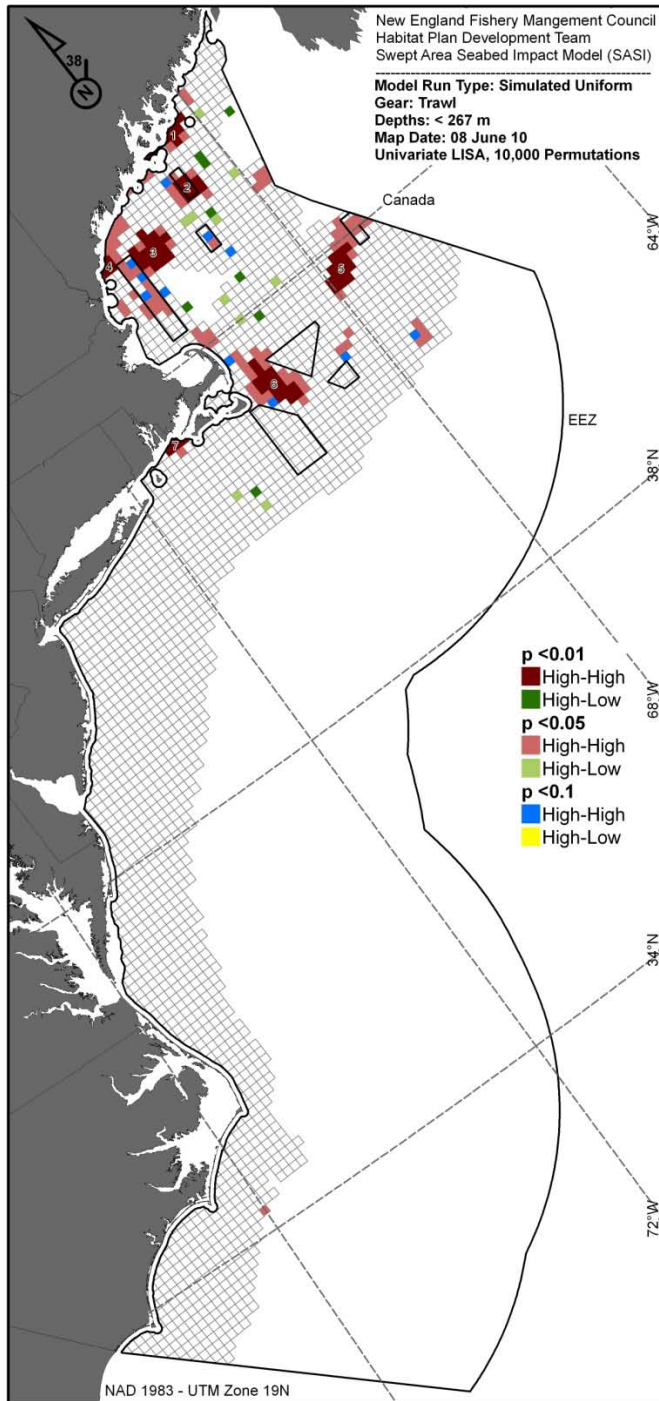
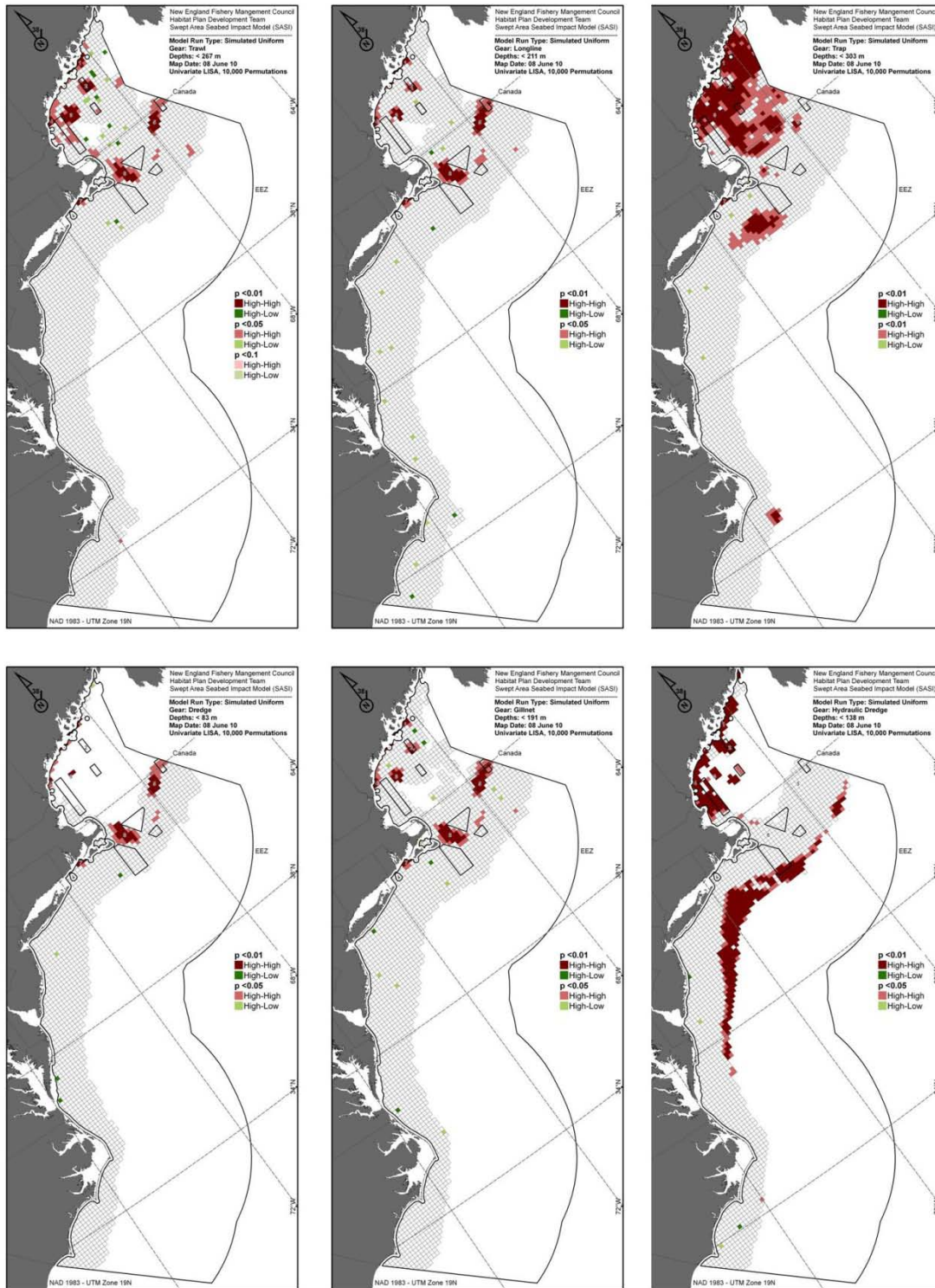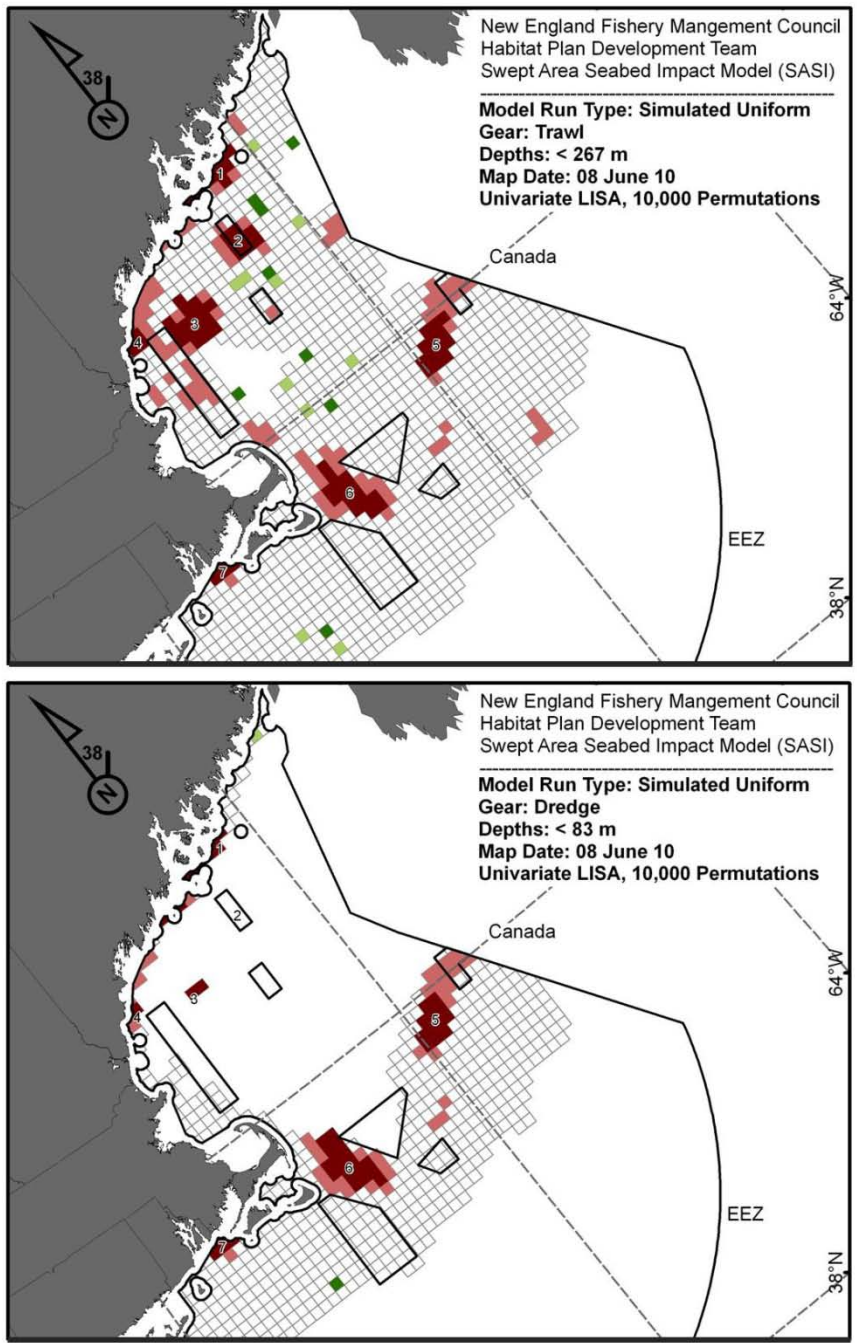**Figure 4 – Maps of z_∞ HH and HL clusters defined by $p \leq 0.05$ and 0.01 levels for each gear type.**

Figure 5 – Maps of z_∞ HH and HL clusters defined by $p \le 0.05$ and 0.01 levels for each trawl and scallop dredge gears.

z∞ in Present and Proposed Management Areas

Methods

Equal Area Permutation (EAP) tests were used to determine the levels of z_∞ in present and proposed management areas relative to the model domain. The area-weighted mean z_∞ ($\overline{z_w^\infty}$) for each tested area was compared to a permutation distribution of $\overline{z_w^\infty}$ calculated using 9,999 randomly placed areas equal in size to the test area. The percentile of the tested area's $\overline{z_w^\infty}$ value and number of areas with $\overline{z_w^\infty}$ greater than or equal to the tested area were identified. These permutation-based areas were mapped along with the 100 highest $\overline{z_w^\infty}$ value areas (99th percentile of the permutations distribution) to indicate alternative management area locations.

The shapes and orientations of the tested areas vary depending on their locations and original management objectives. Circles were used to construct consistent permutation distributions for the EAP tests because they are isotropic and their areas can calculated simply using radii (Area = 2π x raduis^2).

Results

The EAP results for trawl gear are summarized in Table 4. On the following pages, results from the CAI S GF EFH area are illustrated in a histogram (Figure 6) and on a map (Figure 7). The histogram indicates the position of the area in its respective EAP distribution, and the map shows the locations of the permutation areas with $\overline{z_w^\infty}$ ≥ than the tested areas, and also the 99th percentile of the $\overline{z_w^\infty}$ permutation values (i.e. the locations of the highest 100 $\overline{z_w^\infty}$ permutation values). Histograms and maps for the other areas listed in Table 4 are not shown.

Table 4 – Trawl EAP results with tested areas, their size, $\overline{z_W^\infty}$ permutation percentile (P%) and number of permutation areas with $\overline{z_W^\infty}$ ≥ than the tested area.

	Closed Area	km²	AWM z∞	Sum z∞	P%	Areas with ≥ Mean z∞	99th %
		Tested area result			**Permutation results**		
Groundfish (Amendment 13) EFH Closed Areas	Cashes L. EFH GF	443	51.437	588.06	96.00%	400	57.661
	Jeffreys B. EFH GF	499	57.667	510.13	99.10%	90	57.101
	WGOM EFH GF	2272	50.114	1777.55	95.10%	490	52.63
	CAII EFH GF	641	49.425	844.79	92.20%	780	56.567
	CAI N. EFH GF	1937	45.186	1287.93	12.80%	8721	53.15
	CAI S. EFH GF	584	46.085	609.67	50.30%	4970	57.101
	NLCA EFH GF	3387	46.787	2205.24	56.80%	4320	51.884
Multispecies mortality closures	Cashes L. Closed Area	1373	48.505	1186.07	83.00%	1700	54.314
	WGOM Closed Area	3030	49.874	2362.75	94.70%	530	52.037
	Closed Area II	6862	46.338	4354.63	41.10%	5891	50.912
	Closed Area I	3939	45.891	2556.1	34.20%	6581	51.589
	Nantucket Lightship	6248	46.466	4002.39	46.30%	5371	51.015

Figure 6 – Trawl EAP histogram for CAI South EFH Groundfish Closed Area indicating the position of the tested area in the EAP distribution (dashed line), the $\overline{z_W^{\infty}}$ (mean z∞) and permutation percentile (P%).
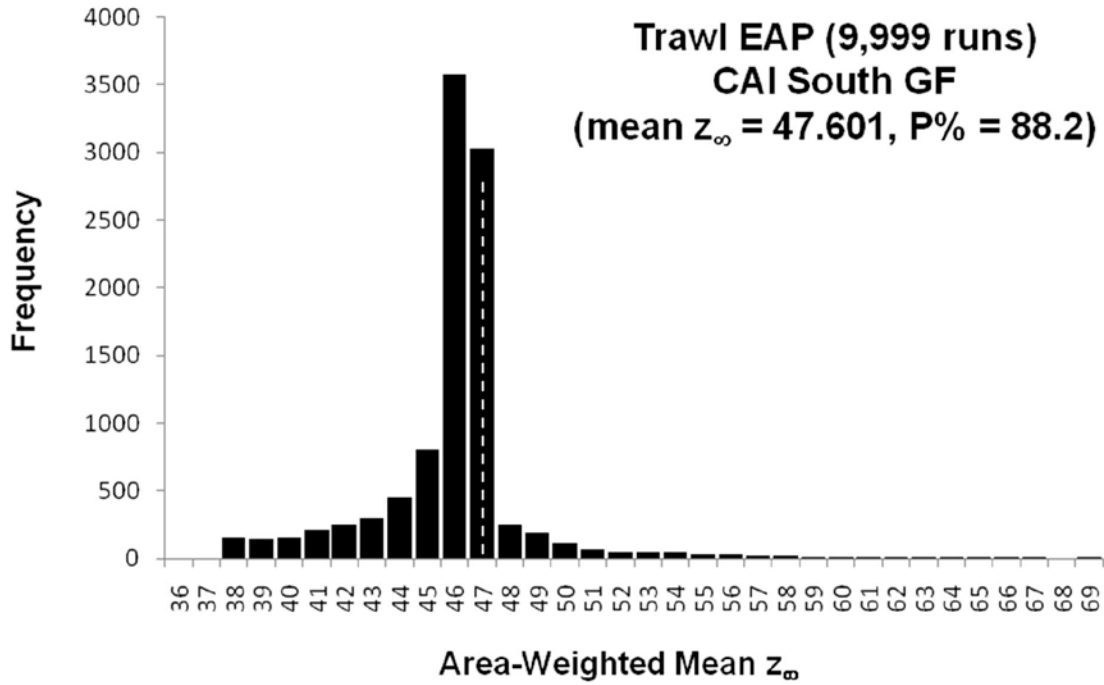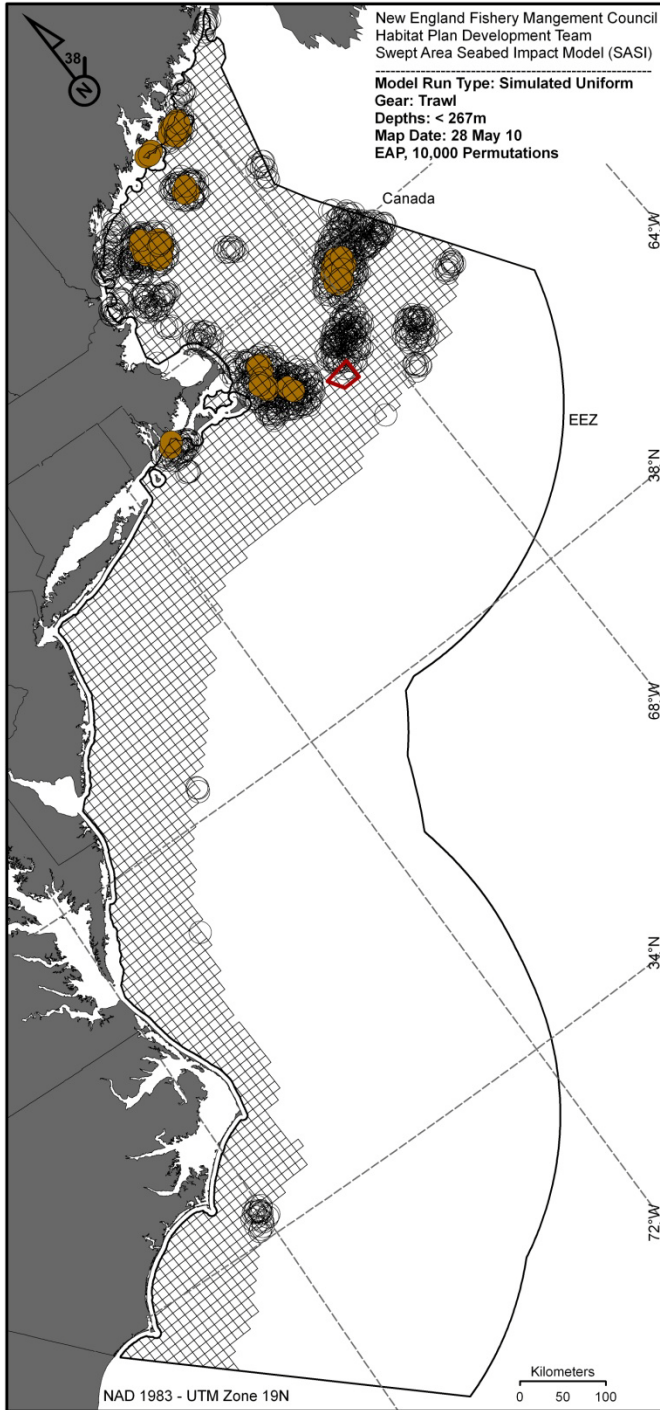
Figure 7 – Trawl EAP map for CAI South EFH Groundfish Closed Area. Open circles are permutation areas with $\overline{z_W^m}$ ≥ than the tested area, and orange circles show the locations of the highest 100 $\overline{z_W^m}$ permutation values.

REFERENCES*

Anselin, L. (1995). "Local Indicators of Spatial Association- LISA." Geographical Analysis 27(2): 93-115.

Anselin, L., 1996. The Moran scatterplot as an ESDA tool to assess local instability in spatial association, in: Fisher, M., Scholten, H.J., Unwin, D., (Eds.), Spatial analytical perspectives on GIS. Taylor & Francis, London, pp. 111–125.

Anselin, L., A. K. Bera, et al. (1996). "Simple diagnostic tests for spatial dependence." Regional Science and Urban Economics 26(1): 77-104.

Anselin, L., Syabri, I., Kho, Y., 2006. GeoDa: An Introduction to Spatial Data Analysis. Geographical Analysis 38, 5–22.

Boots, B., 2002. Local measures of spatial association. Ecoscience 9, 168–176.

Cressie, N. 1993. Statistics for spatial data, Revised Edition. Wiley Series in Probability and Statistics, Wiley, New York.

Fortin, M.-J. and M. Dale (2005). Spatial Analysis: a Guide for Ecologists. Cambridge, Cambridge University Press.

Isaaks, E.H., Srivastava, R.M., 1989. An Introduction to Applied Geostatistics. Oxford University Press, Oxford.

Moran, P. A. P. (1950). "Note on Continuous Stochastic Phenomena." Biometrika 37(1-2): 17-23.

Ord, J.K., Getis, A., 1995. Local Spatial Autocorrelation Statistics: Distributional Issues and an Application. Geographical Analysis 27, 286–306.

Ord, J. K. and A. Getis (2001). "Testing for Local Spatial Autocorrelation in the Presence of Global Autocorrelation." Journal of Regional Science 41(3): 411-432.

Sibson, R., 1981. A brief description of natural neighbor interpolation, in: Barnett, V., (Ed.), Interpreting Multivariate Data. Wiley Press, New York, pp. 21–36.

*not all references are cited in the text above